Invited Paper

# Statics and Dynamics of Colloidal Particles in Periodic Traps

C. Reichhardt[a] and C. J. Olson Reichhardt[b]

[a]T-CNLS and T-13, Los Alamos National Laboratory, Los Alamos, NM, USA
[b]T-12, Los Alamos National Laboratory, Los Alamos, NM, USA

## ABSTRACT

We show with computer simulations that a rich variety of static and dynamical colloidal phases can be realized for colloids interacting with two-dimensional periodic substrates. For the static case a new type of colloidal state that we term colloidal molecular crystals occurs when there is an integer number of colloids per substrate minima. Here there is a novel orientational ordering in addition to the positional ordering of the colloids. The colloidal molecular crystals exhibit a multi-step melting in which the orientational ordering is lost first, followed by the positional ordering. This multi-step melting phenomenon agrees well with recent experiments. Additionally we show that at fillings where the number of colloids is an incommensurate fraction of the number of substrate minima, as a function of temperature there is a transition to a state in which local incommensurations become thermally activated. With an applied drive we find that a remarkable number of distinct dynamical phases can be realized, including ordered and disordered flows. We also illustrate flow phases in which the colloidal motion locks to a symmetry direction of the underlying lattice.

**Keywords:** colloids, melting, dynamics, crystals

## 1. INTRODUCTION

There are a wide variety of systems which can effectively be modeled as an assembly of particles interacting with some form of two-dimensional (2D) periodic substrate. Specific examples include atoms or molecules deposited on 2D films,[1] charge density wave systems,[2] vortices in superconductors interacting with periodic arrays of pinning sites[3–6] or magnetic dots,[7–9] and vortices in Bose-Einstein condensates with periodic optical trap arrays. In general, these systems show a rich variety of commensurability phenomena which occur when the number of particles is an integer or rational fraction of the number of substrate sites.[3,4,6–8,10] At these commensurate densities the particles can form highly ordered crystalline structures and exhibit enhanced melting temperatures or enhanced pinning thresholds. At incommensurate fillings the system may be filled with grain boundaries dividing the sample into different regions that are commensurate with the substrate.[6] If the system is close to a strongly commensurate filling, such as near an integer filling, there may be well defined species of interstitials or vacancies in commensurate configurations.[11] Under an applied drive these systems also show a wealth of dynamical phenomena.[11–13] For instance, in sliding charge density wave systems, intricate switching behavior may arise.[2] If an additional ac drive is superimposed with an applied dc drive, a rich phase-locking phenomenon can occur where the intrinsic frequency of the particle velocity moving over the periodic substrate locks with the applied ac frequency.[2,13] In atom-on-atom problems, transitions from ordered flows to highly disordered flows are possible.[1] For vortices in superconductors with periodic pinning arrays, a series of dynamical phases from ordered soliton flows to strongly fluctuating flows occur as the drive is increased.[11] Additionally it is possible to observe symmetry locking effects as the angle of drive is varied with respect to the symmetry direction of the underlying crystal[12]; here, the particles preferentially flow along the stronger symmetry direction. In most of the experimentally realizable systems of these types, the microscopics of the individual particle motions or positions can not be accessed accessed directly, and instead changes are observed in bulk measurements such as critical current, magnetization, or the friction coefficient.

Recently, another type of system of interacting particles on a 2D periodic substrate has been realized experimentally in the form of colloidal particles on periodic optical traps.[15–23] A particular advantage of this system

Further author information:
C.R.: E-mail: charlesr@cnls.lanl.gov, Telephone: 1 505 665 0059
C.J.O.R.: E-mail: cjrx@lanl.gov, Telephone: 1 505 665 1134



Optical Trapping and Optical Micromanipulation, edited by
Kishan Dholakia, Gabriel C. Spalding, Proceedings of SPIE Vol. 5514
(SPIE, Bellingham, WA, 2004) · 0277-786X/04/$15 doi: 10.1117/12.558964

over those mentioned above is that, due to the micron size scale of the colloids, it is possible to directly visualize the individual particles using video-microscopy. The colloidal particles are ideal as a model condensed matter system, and in addition, there are a number of potential applications for colloids on periodic substrates. The ability to make tailored ordered colloidal crystals in an efficient manner can be very valuable for the creation of photonic band gap materials. Additionally, it has been proposed that by driving colloids over periodic substrates, new types of sorting devices can be made in which one species of colloid moves along a symmetry direction of the periodic substrate while other species do not, so that over time the colloid species are separated laterally in space.[18, 20, 21]

## 2. SIMULATION

We consider a two-dimensional system with periodic boundary conditions in the $x$ and $y$ directions. We model $N_c$ colloids interacting with a repulsive screened Coulomb interaction, and we add thermal noise to our system. There is a periodic substrate with square or triangular symmetry and $N_p$ potential minima, giving a filling fraction of $N_c/N_p$. The equation of motion for a single colloid is

$$\eta \mathbf{v} = \mathbf{f}_i = -\sum_{j \neq i}^{N_v} \nabla_i U(r_{ij}) + \mathbf{f}_i^s + \mathbf{f}_i^T. \tag{1}$$

Here $\eta = 1$ is the damping constant and

$$U(r_{ij}) = -\left(\frac{q}{|\mathbf{r}_i - \mathbf{r}_j|}\right) \exp(-\kappa |\mathbf{r}_i - \mathbf{r}_j|) \tag{2}$$

is the colloid-colloid interaction potential. The screening length is $1/\kappa = 3$, $q$ is the charge of the colloids, and $\mathbf{r}_{i(j)}$ is the position of particle $i(j)$. Distances are measured in units of the substrate lattice constant $a_0$. The force from a triangular substrate of strength $A$ is given by

$$\mathbf{f}_i^s = \sum_{k=1}^{3} A \sin\left(\frac{2\pi p_k}{a_0}\right) [\cos(\theta_k)\hat{\mathbf{x}} - \sin(\theta_k)\hat{\mathbf{y}}] \tag{3}$$

where $p_k = x\cos(\theta_k) - y\sin(\theta_k) + a_0/2$, $\theta_1 = \pi/6$, $\theta_2 = \pi/2$, and $\theta_3 = 5\pi/6$. The force from a square substrate is given by

$$\mathbf{f}_i^s = A \sin\left(\frac{2\pi x}{a_0}\right)\hat{\mathbf{x}} + A \sin\left(\frac{2\pi y}{a_0}\right)\hat{\mathbf{y}}. \tag{4}$$

The thermal noise $\mathbf{f}_i^T$ arises from random Langevin kicks with $< f^T(t) >= 0$ and $< f_i^T(t) f_j^T(t') >= 2\eta k_B T \delta_{ij} \delta(t - t')$. We measure temperature in units of the temperature $T_m$ at which the bulk system melts in the absence of a substrate.

## 3. COLLOIDAL MOLECULAR CRYSTALS

We first consider the ground states that can be generated when the number of colloids equals an integer multiple of the number of potential minima in the underlying substrate. To obtain these states, we start the system at a high temperature such that the particles are diffusing randomly, and slowly cool to $T = 0$. We consider the case where the periodicity and strength of the substrate is held fixed and the density of the colloids is varied. In Fig. 1 we show the ground states for $N_c/N_p = 1, 2, 3$, and 4 for the case of a triangular substrate. In Fig. 1(a) each colloid sits in the center of the potential substrate minima forming a commensurate triangular lattice. In Fig. 1(b) each minima now captures two colloids forming a dimer state. There is also a clear orientational ordering of the dimers, with dimers in one row all aligned in the same direction and dimers in the adjacent rows aligned in the other direction. This structure is very similar to the "herringbone" structures observed for molecular dimers deposited on a triangular substrate.[24–26] In Fig. 1(c), each substrate captures three colloids and the colloids form an orientationally ordered trimer state with all the trimers aligned in the same direction. Fig. 1(d) shows the case where four colloids are captured and an ordered diamond state appears. Since

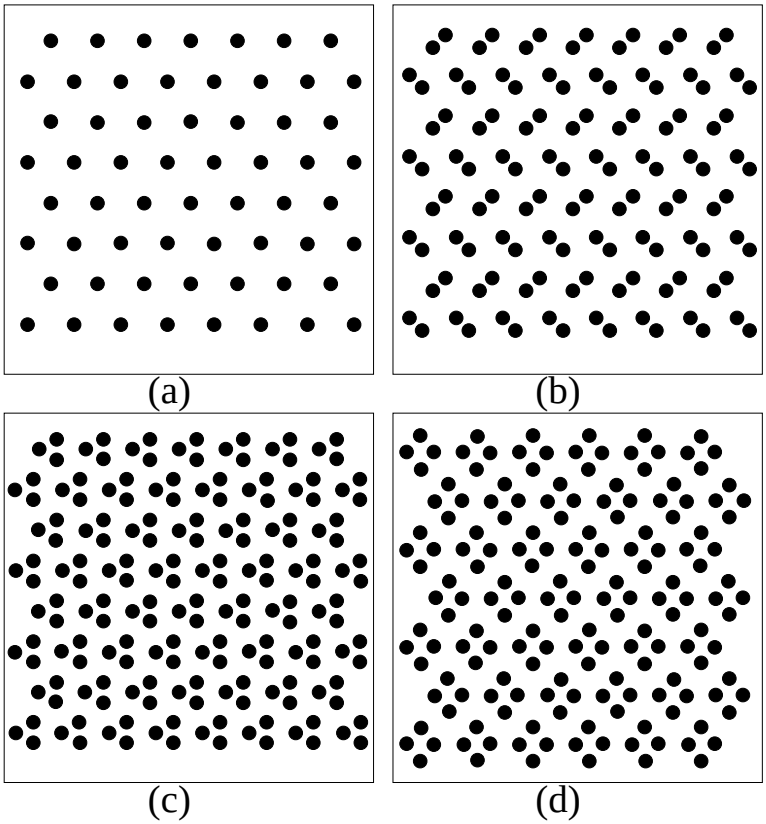


**Figure 1.** Colloidal positions (black dots) for a system with an underlying triangular substrate. (a) One colloid per substrate minima, $N_c/N_p = 1$. (b) Two colloids per substrate minima, $N_c/N_p = 2$. (c) Three colloids per substrate minima, $N_c/N_p = 3$. (d) Four colloids per substrate minima, $N_c/N_p = 4$.

these colloidal crystalline structures have many similarities with molecular crystals, we have termed these states "colloidal molecular crystals." We have also investigated the effect of an underlying square substrate. Here we find orientationally ordered colloidal molecular crystal states, although the particular geometry of the crystals is different.[15] The reason that the dimer, trimer, and higher order states are orientationally ordered is that the colloids in neighboring minima interact with each other through an effective multipole potential which produces anisotropic interactions.

We next consider the melting of the colloidal molecular crystals. We measure both the orientational order of the dimers and trimers as well as the diffusion of the individual particles. In general, we find that if the substrate is sufficiently strong, there is a two-stage melting where the first melting transition is the loss of the orientational ordering of the dimers or trimers. Here the dimers or trimers begin to rotate; however, the colloids remain confined in the potential minima so there is no long time diffusion. For higher temperatures the second stage of the melting occurs, as indicated by the onset of diffusion of individual colloids throughout the entire system. In Fig. 2 we illustrate the melting process for the simplest colloidal molecular system which is the dimer state on a square substrate. In Fig. 2(a), which shows the low temperature phase, the dimers remain orientationally ordered. In Fig. 2(b) at a higher temperature, the orientational ordering of the dimers is lost and the dimers rotate as seen by the lines marking the colloid trajectories. We call this phase a disordered solid. In Fig. 2(c) at a still higher temperature, the individual colloids diffuse throughout the system, although the effect of the substrate is still evident. We call this phase a modulated liquid.

By performing a series of simulations for varied substrate strength $A$ and temperature $T$, we map the onset of the different phases for the system with a square substrate at $N_c/N_p = 2.0$. In Fig. 3 we show the phase diagram

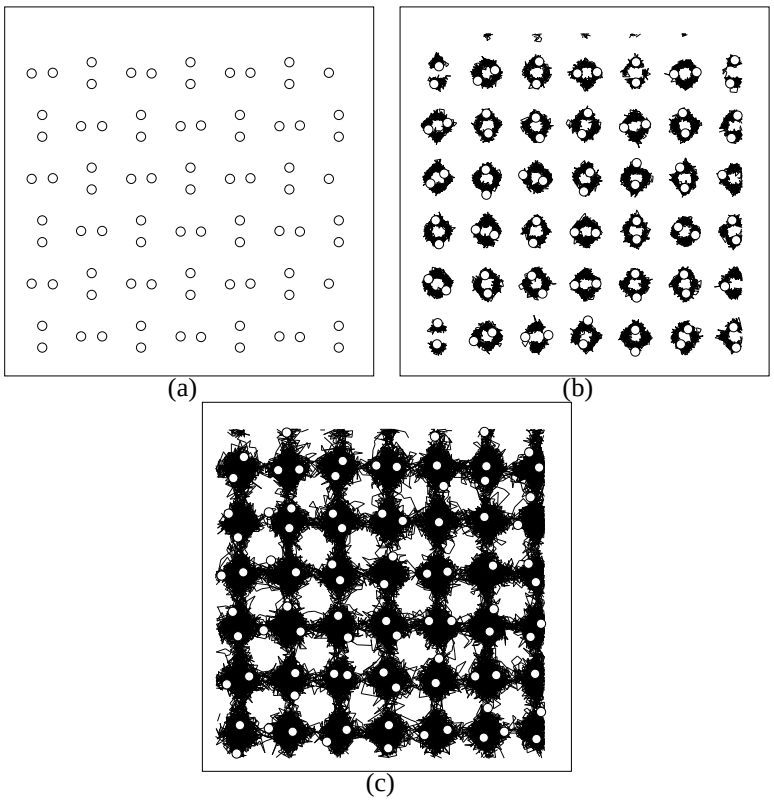


**Figure 2.** Colloidal positions (white dots) and trajectories (black lines) for increasing temperature in a system with a square substrate and two colloids per minima. (a) Ordered solid; (b) disordered solid, (c) modulated liquid.

for this system. Here $T_m$ is the temperature where the colloidal lattice melts in the absence of the substrate. We do not show the phases seen for finite but very weak substrates, where a floating solid appears. For intermediate substrate strengths $A < 2$, the orientationally ordered solid melts directly into the modulated liquid state. For higher substrate strengths $A \geq 2$, the intermediate disordered solid phase appears. The temperature at which the disordered solid melts into the liquid increases with increasing substrate strength. Interestingly, the temperature at which the ordered solid melts to the disordered solid *decreases* with increasing substrate strength. This effect occurs because the orientational ordering of the colloids originates from the effective multipole moment of the dimer interactions. The multipole moment is proportional to the distance $d$ between the two colloids forming the dimer. As the substrate strength increases, the colloids forming the dimer are forced closer to each other and the strength of the multipole moment is reduced, thus reducing the temperature at which the ordering due to the multipole interaction is lost.

The colloidal molecular crystal states illustrated in Fig. 1(c) were recently observed experimentally for a system of colloids interacting with a triangular substrate.[16] These experiments also showed that the orientationally ordered colloidal molecular crystal changes to a disordered solid state as the substrate strength is increased, in agreement with the predictions from the phase diagram in Fig. 3.[15] More recently, a theoretical analysis[22] of the orientational ordering and disordering of the colloidal molecular crystals showed explicitly that it is the multipole moments of the dimers or trimers which give rise to the orientational ordering of the states. It was shown analytically that the ordered solid to disordered solid transition temperature decreases with increasing substrate strength as the distance between the colloids in the dimer or trimer states is reduced. Ref.[22] also showed that the dimer case can be mapped to an anti-ferromagnetic Ising model and that the disordering transition is Ising-like in nature. By changing the anisotropy of the pinning, it should be possible to go from an anti-ferromagnetic limit to a ferromagnetic limit, with interesting glassy states between.

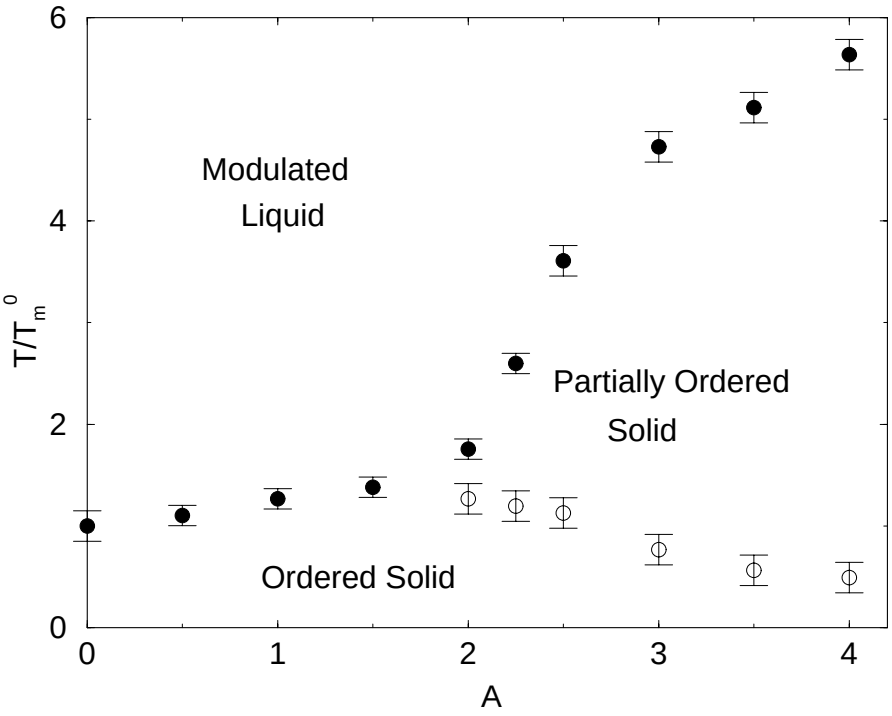


**Figure 3**. Phase diagram of temperature $T$ vs substrate strength $A$ for the dimer system illustrated in Fig. 2.

We next consider incommensuration effects that occur when the number of colloids is not an integer multiple of the number of substrate minima. In Fig. 4 we show the colloidal states at $N_c/N_p = 1.5$ for the square and triangular substrates obtained by annealing from a high temperature. For the square substrate, shown in Fig. 4(a), we find a checkerboard ordering where every other potential minima captures two colloids; however, the long-range orientational ordering of the dimers is lost. This loss of dimer ordering may be due to the increased distance between the dimers, which is now twice as large as it was for $N_c/N_p = 2.0$, and the fact that the multipole interaction strength decreases rapidly as a function of distance. For the triangular substrate shown in Fig. 4(b), we find two types of disordering effects. Not only is there no orientational ordering of the dimers, there is also no ordering of the minima that have captured one rather than two colloids. We note that for a triangular lattice at half filling, the system is geometrically frustrated.

Near the integer matching we obtain localized incommensurations. In Fig. 5(a) we show a system with a triangular substrate for $N_c/N_p = 2.04$, just above the second filling commensurate case, and in Fig. 5(b) we show a filling just below commensuration, $N_c/N_p = 1.96$. In both cases we find clearly defined incommensurations where there is a triply or singly occupied minima surrounded by the dimers. These defects cause a distortion in the surrounding dimer ordering; however, further away from the defects the system maintains the $N_c/N_p = 2.0$ herringbone ordering. In Fig. 5(b), the dimers surrounding the incommensurate singly-filled minima are oriented with the dimer direction pointing toward the incommensurate site in a pinwheel configuration.[27] Conversely, in Fig. 5(a) the dimers surrounding the incommensurate trimers are oriented perpendicularly to the trimer. In each case the dimers act to screen the incommensuration.

Next we consider the melting at fillings near the commensurate states. The simplest case occurs just above the first filling at $N_c/N_p = 1.02$. Here, most of the potential minima capture single colloids, while a few minima which are on average far apart contain two colloids. At $N_c/N_p = 1.02$ there is a well defined melting transition to a liquid state, and a two stage melting occurs where the first stage is the thermal depinning of the incommensurations. In Fig. 6 we show the colloids (white dots) and the trajectories (black lines) for the system just above the first melting transition. Here clear hops of the incommensurations from one potential minimum to an adjacent minimum occur while the commensurate colloids remain immobile. The onset of the diffusion of

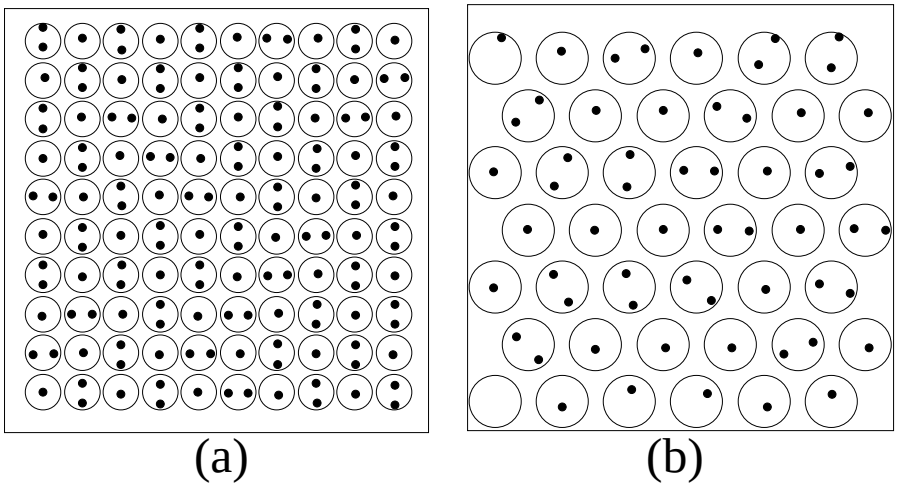


**Figure 4.** Colloidal positions (black dots) for fillings of $N_c/N_p = 1.5$ for (a) square substrate lattice and (b) triangular substrate lattice. The circles are centered at the minima of the substrate.

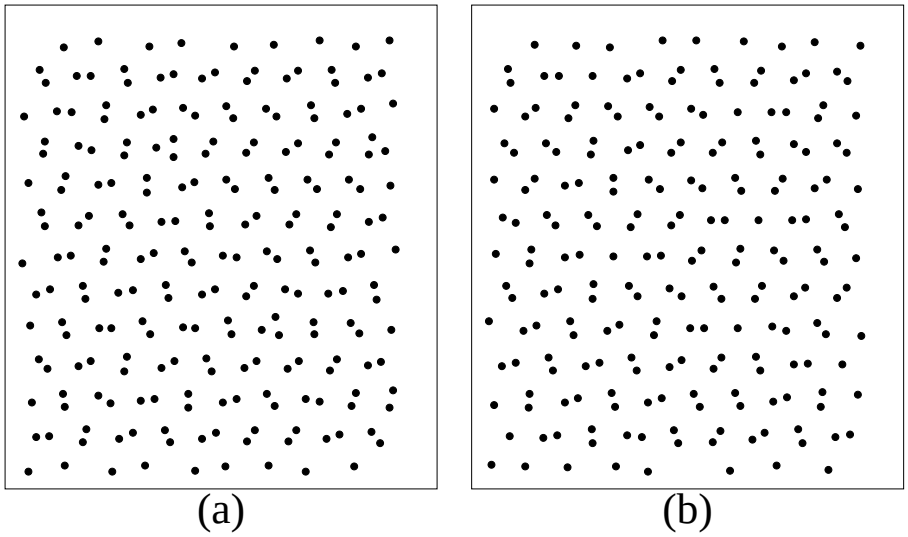


**Figure 5.** Colloidal positions (black dots) for a system with a triangular substrate at fillings of (a) $N_c/N_p = 2.04$, (b) $N_c/N_p = 1.96$.

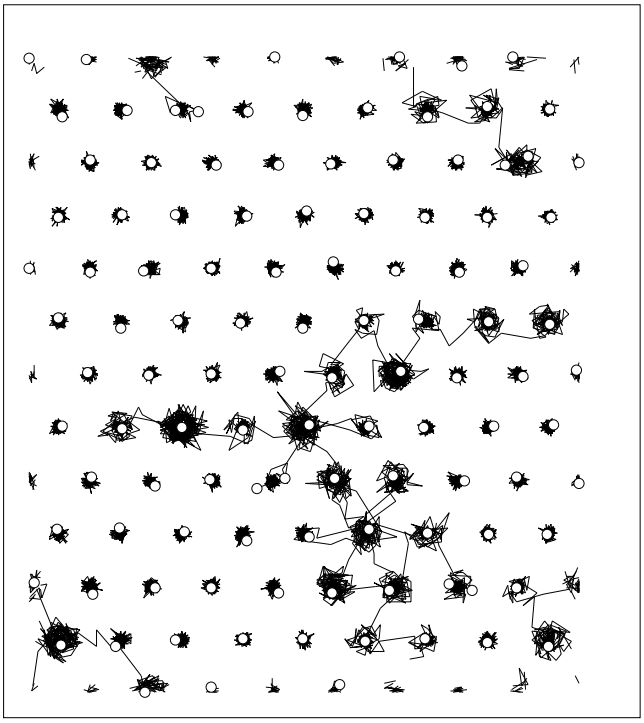

**Figure 6.** Colloidal positions (white dots) and colloidal trajectories (black lines) for a system with a triangular substrate, finite temperature, and a filling of $N_c/N_p = 1.02$.

the incommensurations occurs when one of the colloids in a doubly occupied site gains enough thermal energy to jump into an adjacent minimum. This is equivalent to the dimer state diffusing over the commensurate substrate. This two stage melting is also consistent with the two stage depinning transition observed for these fillings close to commensuration, which we discuss in the next section. As the filling is increased further from commensuration, the two step melting transition becomes increasingly smeared.

We note that below the first commensuration at $N_c/N_p = 1$, a similar two stage melting occurs, only here the vacancies become mobile before the commensurate colloids do. The temperature difference between the two melting stages is much smaller in this case than it is for fillings just above the first commensuration, since the thermal depinning temperature for vacancies is much higher than that of the dimers. Also, near the second commensurate filling, a similar type of two step melting occurs involving vacancies in the dimer lattice (singly occupied sites) at fillings below the commensuration, or the diffusion of isolated trimers at fillings above the commensuration.

## 4. DRIVEN DYNAMICS

We next consider the effect of an applied driving force $f_d$ in the positive $x$ direction on the colloidal molecular crystals. Experimentally this would correspond to an applied electric field. In the simulations, we slowly increase $f_d$ from zero in small increments and measure the average colloidal velocity. In Fig. 7 we plot the velocity vs force curves for (from bottom to top) $N_c/N_p = 1.0, 1.03, 1.09, 1.16, 1.3$, and 1.57.

For the commensurate case $N_c/N_p = 1.0$, there is a well defined sharp threshold where all colloids depin at once. This corresponds to the maximum depinning threshold, since at the first commensurate filling all the forces on a given colloid from the other colloids are exactly balanced due to the symmetry of the colloidal lattice, and the depinning threshold equals the maximum pinning force from the substrate, $A = 1$. At the incommensurate fillings the colloidal configurations are no longer completely symmetric; thus, some colloids experience a net

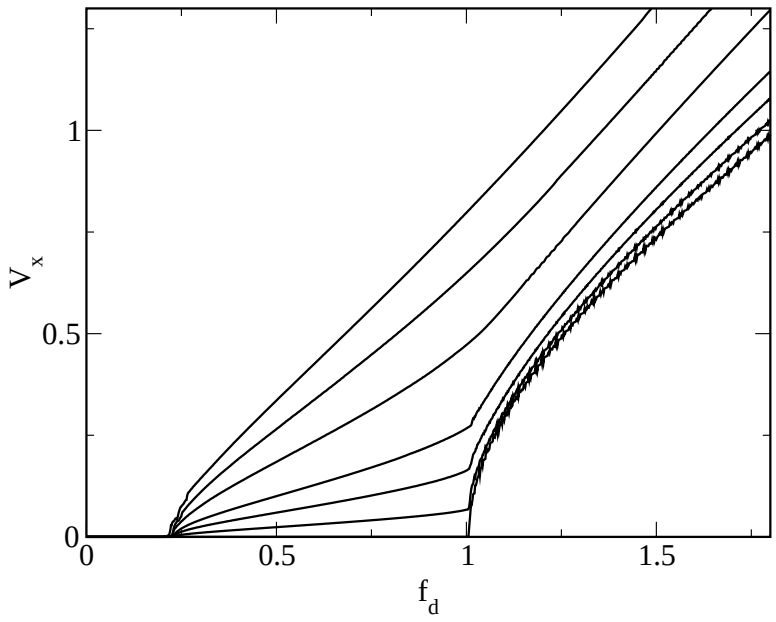


**Figure 7.** Velocity $V_x$ vs applied drive $f_d$ for a system with a triangular substrate at $T = 0$ for fillings $N_c/N_p = 1.0$, 1.03, 1.09, 1.16, 1.3, and 1.57 (from bottom to top).

force from the surrounding colloids that is not balanced by symmetry, and the depinning threshold for these colloids is lowered. For the fillings $N_c/N_p = 1.03, 1.09$, and 1.16, there is a clear two stage depinning process. The first depinning transition involves the incommensurate minima that have captured two colloids rather than one. These dimer sites disturb the surrounding singly occupied minima. A single colloid to the right of a dimer ("downstream" with respect to the applied driving force) experiences a repulsive force from the direction of the dimer that is not counterbalanced by another dimer. As a result, the single colloid is shifted further to the right with respect to the potential minimum than the other single colloids, and it depins before single particles would at the commensurate case $N_c/N_p = 1.0$. The second stage of the depinning transition at $N_c/N_p = 1.03$, when all of the remaining particles depin, occurs very close to the depinning transition at the commensurate case of $N_c/N_p = 1.0$. For higher fillings the two-step depinning process becomes increasingly smeared. At $N_c/N_p = 2.0$ the depinning threshold is sharp and occurs in a single stage as all the colloids depin at once. This is again due to the fact that the colloids form an ordered symmetrical crystal in which the colloid-colloid interactions cancel. For fillings $N_c/N_p > 2.0$ we also find a two stage depinning transition, where the initial depinning occurs for the incommensurations that have three colloids per trap.

In Fig. 8(a) we plot the colloidal trajectories for the $N_c/N_p = 1.03$ case above the first depinning transition. Here the motion occurs in 1D paths along the rows that contain doubly occupied substrate sites. In the rows which are fully commensurate, the colloids remain pinned. In Fig. 8(b), above the second depinning transition, all the rows of colloids are moving and the colloids again follow 1D paths.

For higher filling fractions the initial depinning transition becomes increasingly disordered and the motion is not confined in strictly 1D paths but shows considerable 2D wandering. In this disordered flow phase, the colloids can still be trapped temporarily in the potential minima; however, over time, all colloids take part in the flow. For higher drives there is a transition to a 1D ordered flow phase in which all the colloids align and form a highly anisotropic smectic crystal. In Fig. 9(a) we show the colloidal positions at $f_d = 0.0$ and $N_c/N_p = 1.7$, when a disordered colloidal molecular crystal forms. In Fig. 9(b) we illustrate a snapshot of the moving crystal state at $f_d = 1.2$ where the colloids align into 1D chains. The colloids have a smectic structure: all the colloids are evenly spaced in the $y$-direction, but since each row contains a different number of colloids the colloids are not aligned in the $x$-direction.

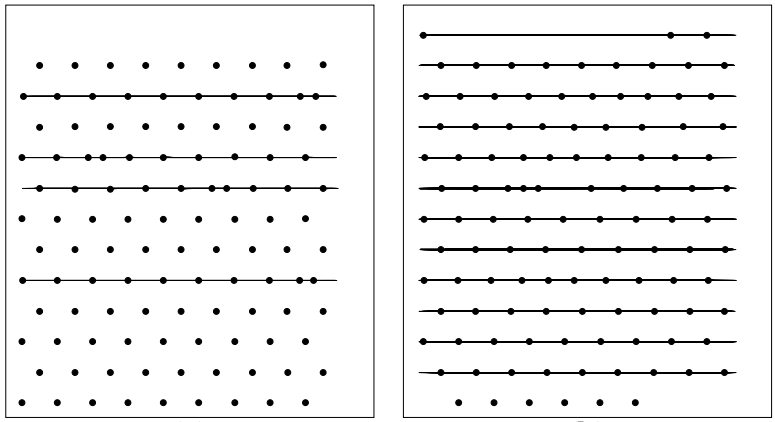


**Figure 8.** The colloid positions (black dots) and colloid trajectories (black lines) for the system in Fig. 7 for a filling fraction of $N_c/N_p = 1.03$ at (a) $f_d = 0.6$ and (b) $f_d = 1.2$.

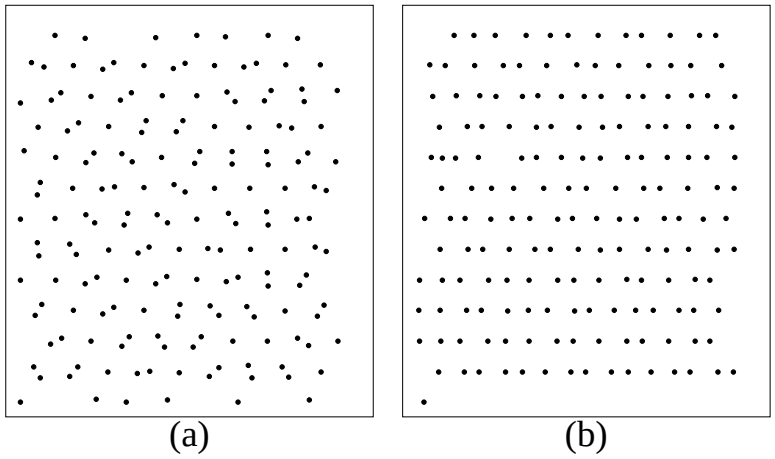


**Figure 9**. The colloid positions (black dots) for a filling fraction of $N_c/N_p = 1.7$ at (a) $f_d = 0.0$ and (b) $f_d = 1.2$.

As the filling fraction is increased further above $N_c/N_p = 2$, the flow becomes increasingly disordered and maintains its 2D character up to higher drives. For filling fractions above 2.5, the high drive flows again reorganize into 1D flow paths which contain two rows of colloids flowing along each substrate row.

## 5. DYNAMICAL SYMMETRY LOCKING

We next consider the case of altering the net direction of drive with respect to the underlying periodic substrate. Simulations for vortices in periodic pinning arrays have shown that the vortex motion locks to certain highly symmetric directions of the underlying substrate.[12] Along these directions, the motion is highly ordered and forms 1D channels. Along the incommensurate angles, the vortex motion is more disordered. Recent experiments with colloids have found similar locking effects.[18,20] Here we consider a system with a triangular substrate where a fixed driving force is applied in the $y$ direction and the drive in the $x$-direction is gradually increased. The net applied force is then $f_d = ((f_d^y)^2 + (f_d^x)^2)^{1/2}$ . The angle of drive with respect to the substrate lattice is $\theta = \arctan(f_y^d/f_x^d)$. In Fig. 10 we plot $V_x$ vs $f_x^d$ for the case of $N_c/N_p = 0.185$ (bottom curve), $N_c/N_p = 0.65$ (middle curve) and $N_c/N_p = 1.57$ (top curve). In the absence of a substrate, $V_x$ increases linearly with $f_d^x$. For $N_c/N_p < 1.0$, there is a clear step region centered around $f_d^x = 0.5$ where $dV_x/df_d^x = 0.0$. Additionally there are some smaller step regions at higher $f_d^x$. The large step corresponds to drives for which the colloids channel along the 60° symmetry direction of the triangular substrate. In this locked phase, the colloids persistently move along the symmetry direction of the substrate in spite of the fact that this is not the direction of the net applied force over most of the step. The higher order steps correspond to a similar locking effect at other symmetry directions. The width of the step is reduced for the $N_c/N_p = 0.65$ case due to the increased colloid-colloid interactions which introduce some disorder. For the case of $N_c/N_p = 1.57$, the step region is replaced with a region of reduced but nonzero slope, although there is still a small step where complete locking occurs. In the reduced slope portion of the curves, incomplete locking of the colloids occurs. Here the colloids move for a period of time along the symmetry direction, but this motion is broken by periods of more disordered flow. As the filling fraction is increased further away from commensuration, the width of the locking regions is further reduced due to the fact that the increased colloid-colloid interactions tend to reduce the effectiveness of the substrate symmetry. The locking effects can be enhanced by increasing the strength of the substrate potential.

In Fig. 11(a) we show the colloid trajectories just before locking for the system with $N_c/N_p = 0.65$. Here some of the colloids channel along the 60° direction; however, there is still considerable motion in the positive $y$-direction. In Fig. 11(b) along the complete locking step, the colloidal motion is in 1D channels along 60°. As the drive is further increased in the $x$-direction, the motion remains locked to the 60° symmetry direction. The trajectories are again disordered when the system exits the locking region for higher drives in the $x$-direction.

We note that the devil's staircase velocity-force curve structures seen in simulations for vortices and in experiments for colloids were obtained on a different type of substrate than that considered here. In the previous work the particles moved over a muffin-tin potential where the pinning sites had a radius $r_p$ which was smaller than the periodicity of the substrate lattice $a$. In the case we consider here, there are no well defined individual pinning sites; instead, the substrate takes the form of an egg-carton potential. The vortex simulations showed that as $r_p$ increased toward $a$, fewer steps appeared on the velocity-force curves and the most prominent steps grew in width, consistent with the results we observe here for the egg-carton potential.

## 6. CONCLUSION

We have investigated the statics and dynamics of colloids interacting with two-dimensional periodic substrates. For the static case we find novel colloidal crystalline structures that we call colloidal molecular crystals, where more than one colloid can be trapped at a single substrate potential minimum. In this case the colloids can act as dimers, trimers, or quadrimers, and they have an orientational ordering as well as a positional ordering. We find that colloidal molecular crystals exhibit a multi-step melting, where for large substrate strengths the orientational ordering is lost while the colloids remain confined within the potential minima. For higher temperatures diffusion of the individual colloids throughout the sample in a modulated liquid state occurs. We also find that the transition temperature from the orientationally ordered colloidal molecular crystals to the disordered colloidal molecular crystal decreases with increasing substrate strength, in agreement with experiment and recent theory. Additionally we find that for incommensurate fillings that are not too far away from integer fillings, there is a

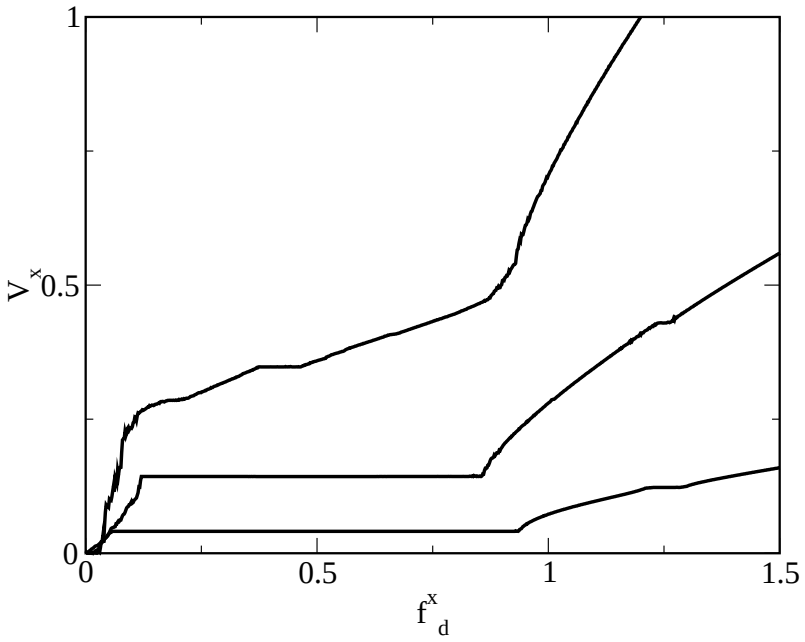


**Figure 10.** The velocity in the $x$-direction vs applied drive in the $x$-direction $f_d^x$ for a system with a fixed force in the $y$-direction. The underlying substrate is triangular. The different curves are for varied filling fraction. From bottom to top, $N_c/N_s = 0.185, 0.65$ and 1.57.

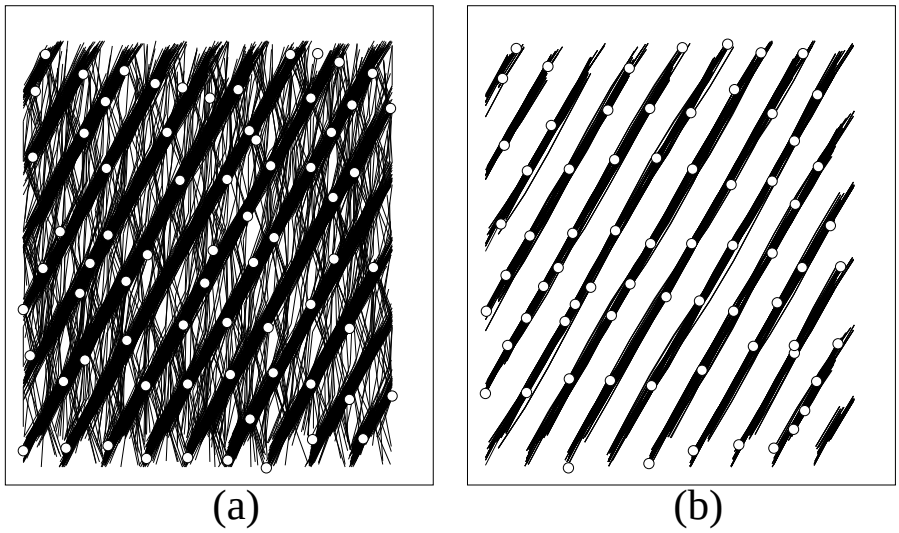


**Figure 11.** The colloidal positions (white dots) and trajectories (black lines) for the system in Fig. 10 at a filling fraction of $N_c/N_p = 0.65$. (a) Just before the main locking step at $f_d^x = 0.1$. (b) Along the main locking step at $f_d^x = 0.5$.

transition temperature above which the incommensurations start to diffuse while the commensurate background remains pinned. We also discuss how colloidal molecular crystal systems may be used as a realization of standard canonical statistical mechanics models.

When the colloidal molecular crystals are driven with an applied uniform force, a series of dynamical phases appear. For incommensurate fillings, a two-stage depinning transition occurs in which the incommensurations depin first, followed by a transition to a disordered flow phase in which all of the particles move. At higher drives the system organizes into a moving smectic state with all the colloids moving in well defined one-dimensional channels which may contain different numbers of colloids. For fillings greater than two the smectic state does not form. We find that the colloidal motion can lock to certain symmetries of the underlying substrates when the direction of the drive is varied. For certain initial directions of drive there are two degenerate symmetry directions and the colloidal motion exhibits a spontaneous symmetry breaking with the global flow following one of the symmetry directions.

## ACKNOWLEDGMENTS

This work was supported by the US Department of Energy under Contract No. W-7405-ENG-36.

## REFERENCES

1. B.N.J. Persson, " Theory and simulation of sliding friction," *Phys. Rev. Lett.* **71**, pp. 1212–1215, 1993.
2. G. Grüner, "The dynamics of charge-density waves," *Rev. Mod. Phys.* **60**, pp. 1129–1181, 1988.
3. M. Baert, V.V. Metlushko, R. Jonckheere, V.V. Moshchalkov, and Y. Bruynseraede, "Composite flux-line lattices stabilized in superconducting films by a regular array of artificial defects," *Phys. Rev. Lett.* **74**, pp. 3269–3272, 1995.
4. K. Harada, O. Kamimura, H. Kasai, T. Matsuda, A. Tonomura, and V.V. Moshchalkov, "Direct observation of vortex dynamics in superconducting films with regular arrays of defects," *Science* **274**, pp. 1167–1170, 1996.
5. S.B. Field, S.S. James, J. Barentine, V. Metlushko, G. Crabtree, H. Shtrikman, B. llic, and S.R.J. Brueck, "Vortex configurations, matching and domain structures in large arrays of artificial pinning centers," *Phys. Rev. Lett.* **88**, pp. 067003/1–4, 2002.
6. A.N. Grigorenko, S.J. Bending, M.J. Van Bael, M. Lange, V.V. Moshchalkov, H. Fangohr, and P.A.J. de Groot, "Symmetry locking and commensurate vortex domain formation in periodic pinning arrays," *Phys. Rev. Lett.* **90**, pp. 237001/1–4, 2003.
7. J.I Martín, M. Velez, J. Nogues, and I.K. Schuller, "Flux pinning in a superconductor by an array of submicrometer magnetic dots," *Phys. Rev. Lett.* **79**, 1929–1932, 1997.
8. D.J. Morgan and J.B. Ketterson, "Asymmetric flux pinning in a regular array of magnetic dipoles," *Phys. Rev. Lett.* **80**, pp. 3614–3617, 1998.
9. J.I. Martín, M. Velez, A. Hoffmann, I.K. Schuller, and J.L. Vicent, "Artificially induced reconfiguration of the vortex lattice by arrays of magnetic dots," *Phys. Rev. Lett.* **83**, pp. 1022–1025, 1999.
10. C. Reichhardt, C.J. Olson, and F. Nori, "Commensurate and incommensurate vortex states in superconductors with periodic pinning arrays," *Phys. Rev. B* **57**, pp. 7937–7943, 1998.
11. C. Reichhardt, C.J. Olson, and F. Nori, "Dynamic phases of vortices in superconductors with periodic pinning," *Phys. Rev. Lett.* **78**, pp. 2648–2651, 1997.
12. C. Reichhardt and F. Nori, "Phase locking, devil's staircases, Farey trees, and Arnold tongues in driven vortex lattices with periodic pinning," *Phys. Rev. Lett* **82**, pp. 414–417, 1999.
13. C. Reichhardt, R.T. Scalettar, G.T. Zimányi, and N. Grønbech-Jensen, "Phase-locking of vortex lattices interacting with periodic pinning," *Phys. Rev. B.* **61**, pp. 11914–11917, 2000.
14. C. Reichhardt, C.J. Olson, R.T. Scalettar, and G.T. Zimányi, "Commensurate and incommensurate vortex lattice melting in periodic pinning arrays," *Phys. Rev. B* **64**, pp. 144509/1–9, 2001.
15. C. Reichhardt and C.J. Olson, "Novel colloidal crystalline states on two-dimensional periodic substrates," *Phys. Rev. Lett* **88**, pp. 248301/1–4, 2002.

16. M. Brunner and C. Bechinger, "Phase behavior of colloidal molecular crystals on triangular light lattices," *Phys. Rev. Lett.* **88**, pp. 248302/1–4, 2002.
17. P.T. Korda, G.C. Spalding, and D.G. Grier, "Evolution of a colloidal critical state in an optical pinning potential landscape," *Phys. Rev. B* **66**, pp. 024504/1–4, 2002.
18. P.T. Korda, M.B. Taylor, and D.G. Grier, "Kinetically locked-in colloidal transport in an array of optical tweezers," *Phys. Rev. Lett.* **89**, pp. 129301/1–4, 2002.
19. K. Mangold, P. Leiderer, and C. Bechinger, "Phase transition of colloidal monolayers in periodic pinning arrays," *Phys. Rev. Lett.* **90**, pp. 158302/1–4, 2003.
20. M.P. MacDonald, G.C. Spalding, and K. Dholakia, "Microfluidic sorting in an optical lattice," *Nature* **426**, pp. 421–424, 2003.
21. A. Gopinathan and D.G. Grier, "Statistically locked-in transport through periodic potential landscapes," *Phys. Rev. Lett.* **92**, pp. 130602/1–4, 2004.
22. R. Agra, F. van Wijland, and E. Trizac, "Theory of orientational ordering in colloidal molecular crystals," Phys. Rev. Lett. **93**, 018304/1–4, 2004.
23. C.J. Olson Reichhardt and C. Reichhardt, "Frustration and melting of colloidal molecular crystals," *J. Phys. A.* **36**, pp. 5841–5845, 2003.
24. A.J. Berlinsky and A.B. Harris, "Orientational phases of hydrogen molecules on a triangular lattice," *Phys. Rev. Lett.* **40**, pp. 1579–1582, 1978.
25. R.D. Diehl, M.F. Toney, and S.C. Fain, "Orientational ordering of nitrogen molecular axes for a commensurate monolayer physisorbed on graphite," *Phys. Rev. Lett.* **48**, pp. 177–180, 1982.
26. C. Peters and M.L. Klein, "Structure of axially compressed monolayers of $N_2$ physisorbed on graphite," *Phys. Rev. B* **32**, pp. 6077–6079, 1985.
27. P. Zeppenfeld, J. Goerge, V. Diercks, R. Halmer, R. David, G. Comsa, A. Marmier, C. Ramseyer, and C. Girardet, "Orientational ordering on a corrugated substrate: Novel pinwheel structure for $N_2$ adsorbed on Cu(110)," *Phys. Rev. Lett.* **78**, 1504–1507, 1997.